ADVANCED MATERIALS

Supporting Information

for *Adv. Mater.,* DOI: 10.1002/adma.202107940

A Two-Pathway Model for the Evolution of Colloidal Compound Semiconductor Quantum Dots and Magic-Size Clusters

Yang Li, Nelson Rowell, Chaoran Luan, Meng Zhang, Xiaoqin Chen, and Kui Yu**

Supplementary Information

A Two-Pathway Model for the Evolution of Colloidal Compound Semiconductor Quantum Dots and Magic-Size Clusters

Yang Li,[†] Nelson Rowell,[‡] Chaoran Luan,[ζ] Meng Zhang,[§] Xiaoqin Chen,[*,†] Kui Yu[*,†,§]

[†]Engineering Research Center in Biomaterials, Sichuan University,
Chengdu, 610065 Sichuan, P. R. China

[‡]Metrology Research Centre, National Research Council Canada,
Ottawa, Ontario K1A 0R6, Canada

[ζ] Department of Ophthalmology, West China School of Medicine,
West China Hospital, Sichuan University, Chengdu,
Sichuan 610065, P. R. China

[§]Institute of Atomic and Molecular Physics, Sichuan University,
Chengdu, 610065 Sichuan, P. R. China

X. C. (email: xqchen@scu.edu.cn) or to K. Y. (email: kuiyu@scu.edu.cn)

Table of Contents

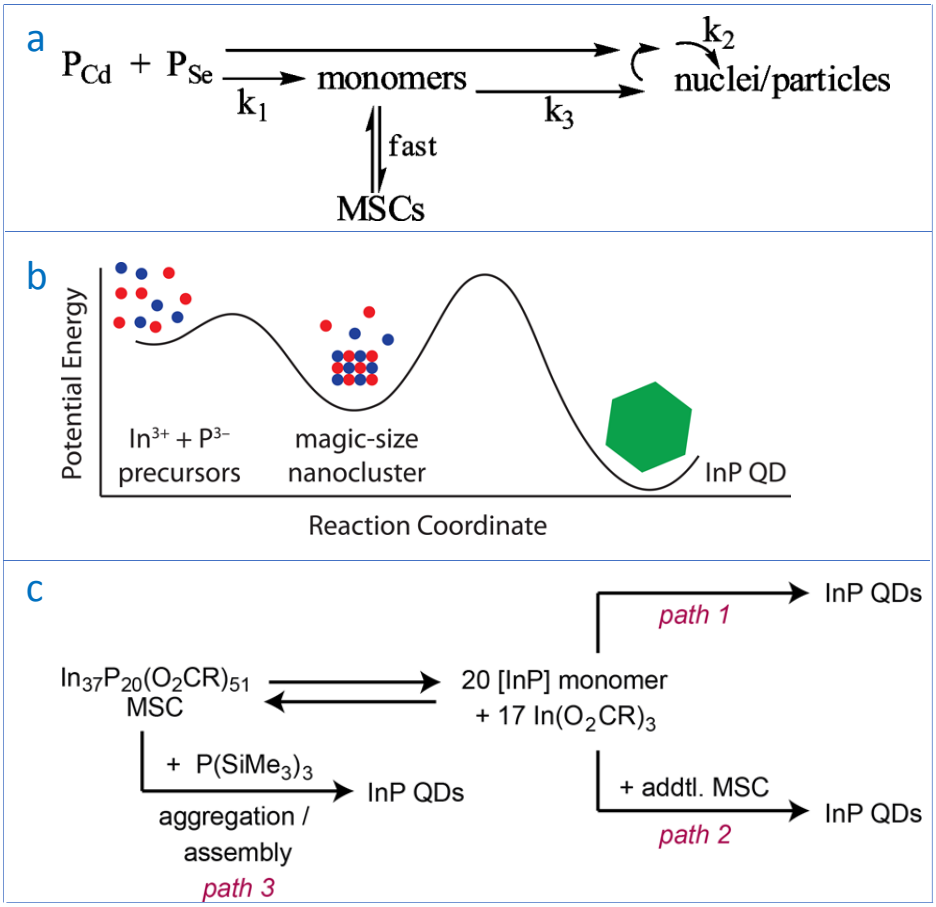

Scheme S1. Growth relation of MSCs to QDs proposed. Part a is Scheme 1 of Ref 9 in the main text,[1] and Parts b and c are about the growth of InP QDs from InP MSCs.[2,3] These three studies suggested that MSCs are a source of monomers for the growth of QDs.[1-3] "The relationship between the **nanoclusters** observed during the nanoparticle synthesis and magic sized clusters has been long recognized."[4] Such a statement, in fact, is consistent with the two-pathway model (Yu) discussed in the present perspective; the **PC** is analogue to the nanoclusters. Moreover, the MSCs can become monomers and fragments via the counterpart precursor compounds (PCs) in two-pathway model (Yu). Since 2017, we have been developing and testing this two-pathway model (Yu) with a completely new synthetic approach. We stop a reaction in its prenucleation stage, which is also called induction period (IP), and use the resulting IP samples to synthesize magic-size clusters (MSCs) and quantum dots (QDs) at low temperatures such as room temperature. This unprecedent approach is innovative with much higher control. The two-pathway model is proposed based on the experimental investigations

on various ME systems (M = Zn and Cd, E = S, Se, and Te). For example, Part 3.1 introduces Ref 56 “Fragmentation of Magic-Size Cluster Precursor Compounds into Ultrasmall CdS Quantum Dots with Enhanced Particle Yield at Low Temperatures”.[5] The abstract of this study says “…Our findings introduce a new approach to making small-size QDs without the coexistence of the PC and with improved particle yield. Providing experimental evidence for the two-pathway model proposed for the pre-nucleation stage of colloidal binary QDs, the present study aids in the advance of non-classical nucleation theory.” Until now, no experimental evidence disputing the model has been encountered. In our view, it usually takes time for a new concept to be fully tested and applied. It usually takes time for a correct concept to appear and even longer for it to be accepted. It might be of help to recall that Alfred Wegner (1830 – 1930) proposed in 1912 that the continents had moved and were still moving; this theory of continental drift was generally accepted in the 1950s and 1960s. Time will certainly provide an answer as to whether the two-pathway model will be widely accepted.

[1] Z. Jiang, D. F. Kelley, Role of Magic-Sized Clusters in the Synthesis of CdSe Nanorods, *ACS Nano* **2010**, *4*, 1561−1572.

[2] D. C. Gary, M. W. Terban, S. J. L. Billinge, B. M. Cossairt, Two-Step Nucleation and Growth of InP Quantum Dots via Magic-Sized Cluster Intermediates, *Chem. Mater*. **2015**, *27*, 1432−1441.

[3] M. R. Friedfeld, D. A. Johnson, B. M. Cossairt, Conversion of InP Clusters to Quantum Dots. *Inorg. Chem.* **2019**, *58*, 803−810.

[4] J. Lee, J. Yang, S. G. Kwon, T. Hyeon, Nonclassical Nucleation and Growth of Inorganic Nanoparticles, *Nat. Rev. Mater.* **2016**, *1*, 16034.

[5] L. Li, J. Zhang, M. Zhang, N. Rowell, C. Zhang, S. Wang, J. Lu, H. Fan, W. Huang, X. Chen, K. Yu, Fragmentation of Magic-Size Cluster Precursor Compounds into Ultrasmall CdS Quantum Dots with Enhanced Particle Yield at Low Temperatures, *Angew. Chem. Int. Ed.* **2020**, *59*, 12013−12021.

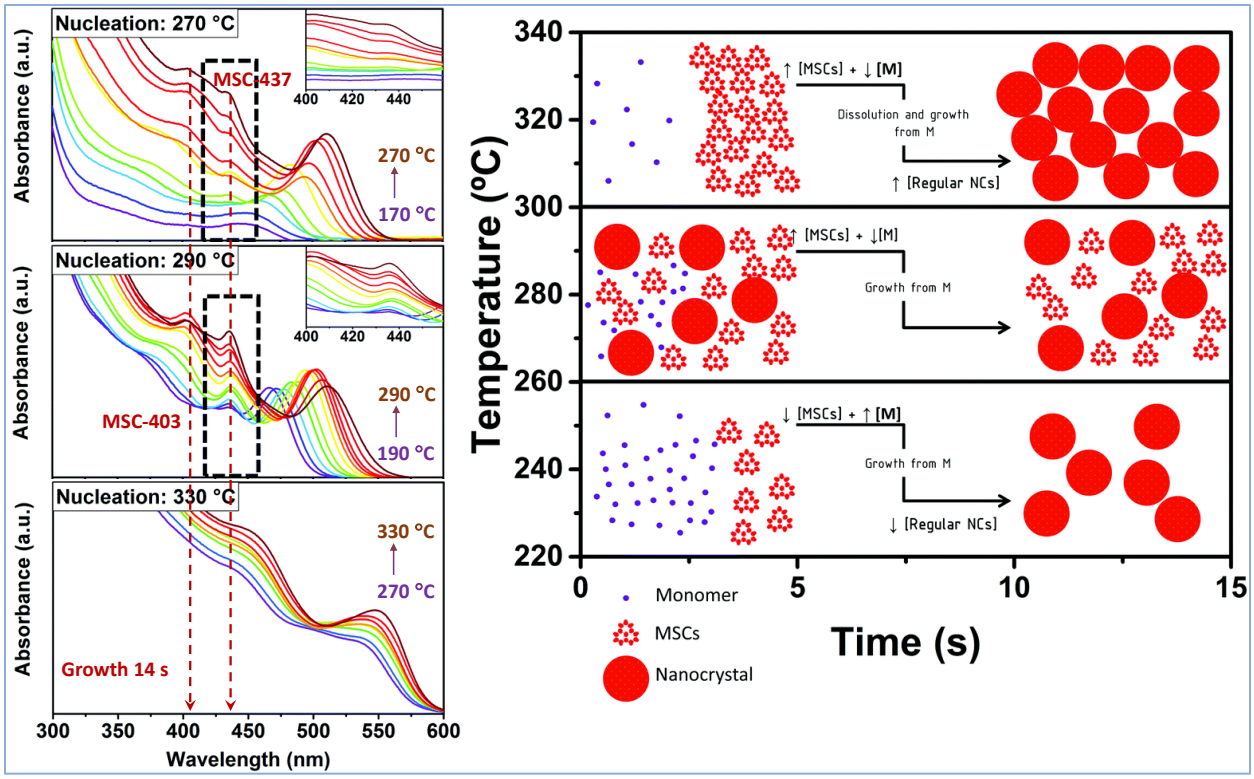

Scheme S2. MSC and QD growth relation derived from **Figure 1** and **Scheme 1** of Ref 10 in the main text. To explain the absorption spectra which were collected (left) during the synthesis of CdSe NCs with a continuous flow cell, the authors developed the scheme (which is depicted on the right) to illustrate the role that MSCs play in the growth of NCs. These authors stated on Page 22932 that

- "At mild temperatures (T ≤ 260 °C) … a high concentration of monomers [M] in solution… these monomers are attached to the smallest MSCs, forming other cluster families… Temperatures above 300 °C induce a high nucleation rate, and consequently the concentration of MSCs formed is high and the monomer concentration is low…"
- "The interplay of reaction parameters creates a small temperature window (260 °C < T ≤ 300 °C) in which the relative reaction rates … MSCs coexist with regular NCs ... Under these conditions, the dissolution of MSCs does not take place, given that the temperatures might not be high enough and that there is no drastic monomer depletion."
- "This NC growth evidences that the monomer availability after nucleation is sufficient for the growth from MSCs into NCs."

We want to point out the complexity of their reaction, notably with regard to the reaction medium of a mixture of TOP and TOPO, the Cd source of $Cd(OAc)_2$, and the octadecylphosphonic acid (ODPA, 99 %) used. The Cd precursors could be resulted from an interaction between Cd and TOP, TOPO, acetate, and ODPA, which have different reactivities towards Se. Thus, it is difficult to extract what might be the effects of the nucleation temperatures, together with the growth temperatures and periods, on the formation of Cd–Se covalent bonds. There appears to be no direct evidence to support the amounts of monomers discussed at the different nucleation and growth temperatures. While this study focused on the post-nucleation period, a continuous redshift in optical absorption spectra was not observed, as would be if the MSCs grew into NCs. Therefore, for this key claimed inference, there is a lack of direct evidence. More experimental efforts would be required, especially with simpler reactions. In a side note, CdSe MSC-415 was not detected, which has been reported elsewhere with and without the presence of CdSe QDs.[1-5] Thus, it is helpful to examine different reactions to study the growth relation between MSCs and QDs, and the nucleation and growth of colloidal semiconductor nanospecies[6,7] from a different prospective with the presence of the PC.

[1] A. Kasuya, R. Sivamohan, Y. A. Barnakov, I. M. Dmitruk, T. Nirasawa, V. R. Romanyuk, V. Kumar, S. V. Mamykin, K. Tohji, B. Jeyadevan, K. Shinoda, T. Kudo, O. Terasaki, Z. Liu, R. V. Belosludov, V. Sundararajan, Y. Kawazoe, Ultra-Stable Nanoparticles of CdSe Revealed from Mass Spectrometry, *Nat. Mater.* **2004**, *3*, 99–102.

[2] M. Zhao, Q. Chen, Y. Zhu, Y. Liu, C. Zhang, G. Jiang, M. Zhang, K. Yu, Precursor Compound Enabled Formation of Aqueous-Phase CdSe Magic-Size Clusters at Room Temperature, *Nano Res.* **2021**, DOI: 10.1007/s12274-021-3858-1.

[3] S. Dolai; P. R. Nimmala; M. Mandal, B. B. Muhoberac, K. Dria, A. Dass, R. Sardar, Isolation of Bright Blue Light-Emitting CdSe Nanocrystals with 6.5 kDa Core in Gram Scale: High Photoluminescence Efficiency Controlled by Surface Ligand Chemistry, *Chem. Mater.* **2014**, *26*, 1278–1285.

[4] K. N. Lawrence, P. Dutta, M. Nagaraju, M. B. Teunis, B. B. Muhoberac, R. Sardar, Dual Role of Electron-Accepting Metal-Carboxylate Ligands: Reversible Expansion of Exciton Delocalization and Passivation of Nonradiative Trap-States in Molecule-Like CdSe Nanocrystals, *J. Am. Chem. Soc.* **2016**, *138*, 12813–12825.

[5] D. Zhu, J. Hui, N. Rowell, Y. Liu, Q. Y. Chen, T. Steegemans, H. Fan, M. Zhang, K. Yu, Interpreting the Ultraviolet Absorption in the Spectrum of 415 nm-Bandgap CdSe Magic-Size Clusters, *J. Phy. Chem. Lett.* **2018**, *9*, 2818–2824.

[6] R. Xie, Z. Li, X. Peng, Nucleation Kinetics vs Chemical Kinetics in the Initial Formation of Semiconductor Nanocrystals, *J. Am. Chem. Soc*. **2009**, *131*, 15457–15466.

[7] S. Abe, R. K. Capek, B. De Geyter, Z. Hens, Reaction Chemistry/Nanocrystal Property Relations in the Hot Injection Synthesis, the Role of the Solute Solubility, *ACS Nano* **2013**, *7*, 943–949.

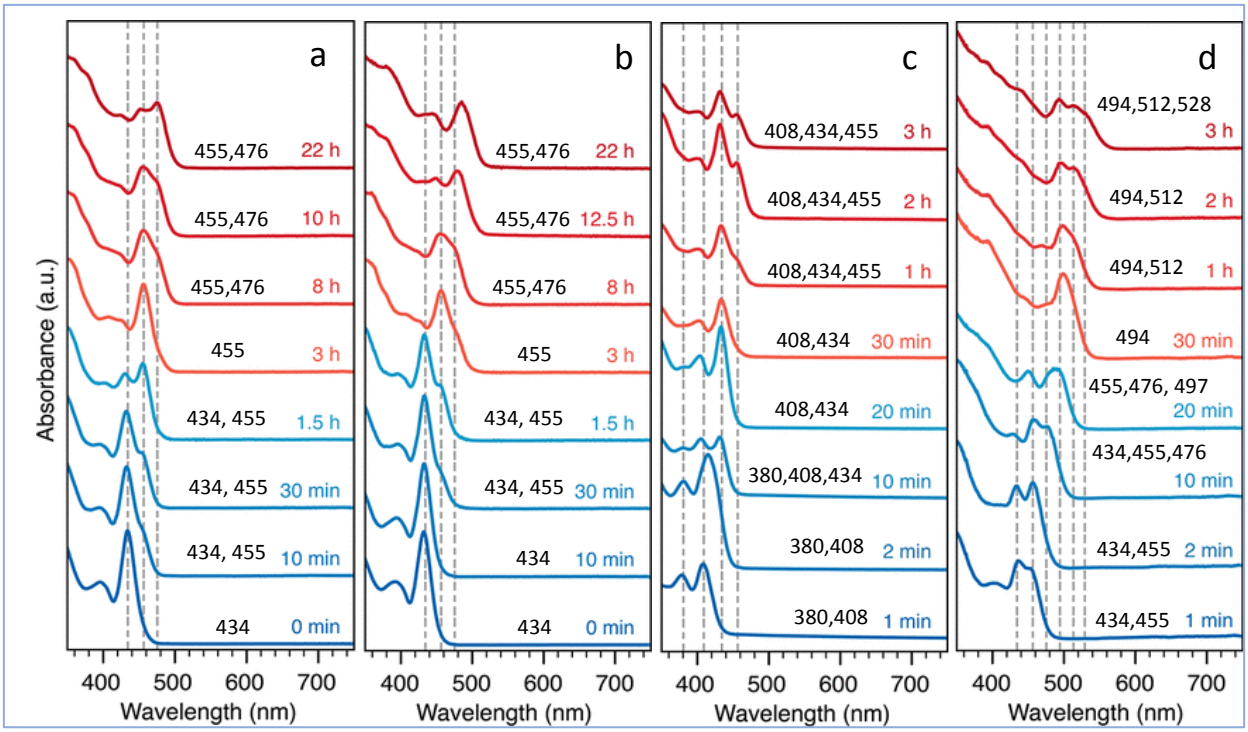

Scheme S3. Derived from **Figures 2** and **6** of Ref 33 in the main text. For the transformation from MSC-434 to MSC-476 via MSC-455 ("Growth of isolated CdSe MSNCs (434)" (a and b)), and from MSC-380, 408, 434, 455, 476, 494, 512/508, and to 528/523 ("Temporal evolution of optical absorption spectra for CdSe MSNC growth" (c and d)), the authors of Ref 33 suggest that

- these clusters have a tetrahedral shape;
- with the addition of a single monolayer (ML) of monomers, the clusters grow in sequence. For the 11 types of MSCs (MSC-355, 380, …, 528/523, 542, and 554), the tetrahedra have the number (n) of Cd atoms on one edge from five to 15, respectively. For example, for MSC-434, this number of n is eight (n = 8);
- transition states are thermodynamically unfavorable and unstable, which were not observed.

Table S1. Literature summary of the composition reported for CdSe MSCs.

Year	Refs	Absorption (nm)–composition	Comments
1990-2009	1	410–$Cd_{35}Se_{16}$	Koch-pyramid tetrahedral shaped fractal growth model
	2	$(CdSe)_{13, 19}$ 415–$(CdSe)_{33/34}$	core-cage structure MS, first-principle calculation
2010-2019	3	$(CdSe)_{19, 33/34}$ 350–$(CdSe)_{13}$	LDI-MS m/z 2488.57 (major) with other peaks
	4	$(CdSe)_{13, 19}$ 418–$(CdSe)_{33/34}$	$(CdSe)_{13}$ major peak LDI-MS m/z 6508
	5	$(CdSe)_{19}$ 418–$(CdSe)_{33/34}$	LDI-MS m/z 6506.5/6314.7 (major)
	6	350–$Cd_{35}Se_{20}$ 380–$Cd_{56}Se_{35}$ 408–$Cd_{84}Se_{56}$	pyramidal nanostructure pair distribution function (PDF)
	7	350–$(CdSe)_{13}$ 419–$(CdSe)_{34}$	ellipsoid-shaped two $(CdSe)_{13}$ paired together
2020-now	8	350–$(CdSe)_{13}$ 380–$(CdSe)_{19}$ 403–$(CdSe)_{33}$ 437–$(CdSe)_{66}$	spherical shape calculated according to *Chem. Mater.* **2003**, *15*, 2854–2860
	9	350–$(CdSe)_{35}$ 380–$(CdSe)_{56}$ 408–$(CdSe)_{84}$ 434–$(CdSe)_{120}$	tetrahedral-shaped layer-by-layer growth of monomers on one of the four identical facets

Effort is need for MSCs to have a better understanding the composition-structure-property relationship.

- CdSe MSCs that display the optical absorption peaking at 350 nm, MSC-350, are reported to be $Cd_{35}Se_{20}$ and $(CdSe)_{35}$ and $(CdSe)_{13}$, with the shape of core-cage, tetrahedral pyramid, and ellipsoid. For MSC-380, $Cd_{56}Se_{35}$ and $(CdSe)_{19}$ and $(CdSe)_{56}$ are assigned.
- "At least four possible structures are proposed for $(CdSe)_{13}$ cluster, namely, core-cage, fullerene-like, wurtzite-like, and paired tubular geometry."[10]
    - pyramidal nanostructure, cadmium benzoate/n-butylamine + bis(trimethylsilyl)

selenide[6]

- ellipsoid, $Cd(OAc)_2$/OA + selenourea[7]
- tetrahedral-shaped, cadmium myristate + bis(stearoyl) selenide[9]

[1] V. Ptatschek, T. Schmidt, M. Lerch, G. Miiller, L. Spanhel, Quantized Aggregation Phenomena in II-VI-Semiconductor Colloids, *Ber. Bunsenges. Phys. Chem.* **1998**, *102*, 85–95.

[2] A. Kasuya, R. Sivamohan, Y. A. Barnakov, I. M. Dmitruk, T. Nirasawa, V. R. Romanyuk, V. Kumar, S. V. Mamykin, K. Tohji, B. Jeyadevan, K. Shinoda, T. Kudo, O. Terasaki, Z. Liu, R. V. Belosludov, V. Sundararajan, Y. Kawazoe, Ultra-stable Nanoparticles of CdSe Revealed from Mass Spectrometry, *Nat. Mater*. **2004**, *3*, 99–102.

[3] Y. Wang, Y. Liu, Y. Zhang, F. Wang, P. J. Kowalski, H. W. Rohrs, R. A. Loomis, M.L. Gross, W. E. Buhro, Isolation of the Magic-Size CdSe Nanoclusters [$(CdSe)_{13}$(n-octylamine)$_{13}$] and [$(CdSe)_{13}$(oleylamine)$_{13}$], *Angew. Chem. Int. Ed.* **2012**, *51*, 6154-6157.

[4] Y. Wang, Y. Zhang, F. Wang, D. E. Giblin, J. Hoy, H. W. Rohrs, R. A. Loomis, W. E. Buhro, The Magic-Size Nanocluster $(CdSe)_{34}$ as a Low-Temperature Nucleant for Cadmium Selenide Nanocrystals; Room-Temperature Growth of Crystalline Quantum Platelets, *Chem. Mater.* **2014**, *26*, 2233–2243.

[5] S. Dolai, P. R. Nimmala, M. Mandal, B. B. Muhoberac, K. Dria, A. Dass, R. Sardar, Isolation of Bright Blue Light-Emitting CdSe Nanocrystals with 6.5 kDa Core in Gram Scale: High Photoluminescence Efficiency Controlled by Surface Ligand Chemistry, *Chem. Mater.* **2014**, *26*, 1278–1285.

[6] A. N. Beecher, X. Yang, J. H. Palmer, A. L. LaGrassa, P. Juhas, S. J. L. Billinge, J. S. Owen, Atomic Structures and Gram Scale Synthesis of Three Tetrahedral Quantum Dots, *J. Am. Chem. Soc.* **2014**, *136*, 10645–10653.

[7] T. Hsieh, T. Yang, C. Hsieh, S. Huang, Y. Yeh, C. Chen, E. Li, Y. Liu, Unraveling the Structure of Magic-Size $(CdSe)_{13}$ Cluster Pairs, *Chem. Mater.* **2018**, *30*, 5468–5477.

[8] C. Palencia, R. Seher, J. Krohn, F. Thiel, F. Lehmkühler, H. Weller, An In Situ and Real Time Study of the Formation of CdSe NCs, *Nanoscale* **2020**, *12*, 22928–22934.

[9] A. S. Mule, S. Mazzotti, A. A. Rossinelli, M. Aellen, P. T. Prins, J. C. van der Bok, S. F. Solari, Y. M. Glauser, P. V. Kumar, A. Riedinger, D. J. Norris, Unraveling the Growth Mechanism of Magic-Sized Semiconductor Nanocrystals, *J. Am. Chem. Soc*. **2021**, *143*, 2037–2048.

[10] M. S. Bootharaju, W. Baek, S. Lee, H. Chang, J. Kim, T. Hyeon, Magic-Sized Stoichiometric II–VI Nanoclusters, *Small* **2021**, *17*, 2002067.

Table S2. Summary of the studies reported on PC characterization.

Year, Journal Ref	Comments
CdTe PC-371, MSC-371 **2017**, *8*, 15467. *Nat. Commun.* Ref. 45	• IP samples (130 °C/30 min) without purification from the $Cd(OAc)_2$/OLA + TeTOP reaction in OLA • Synchrotron-based SAXS, similar sizes, the existence of the PC in the IP sample • ESI-MS, Cd_xTe_y fragments, the PC has Cd–Te bonds • ^{31}P and ^{113}Cd NMR, the self-assembly and Cd–Te bond formation
CdS PC-311, MSC-311 **2017**, *29*, 5727−5735. *Chem. Mater.* Ref. 40	• IP samples without purification from the $Cd(OA)_2$ + S reaction in ODE • MALDI-TOF MS, similar peak positions at ~5167 Da, a pair of quasi isomers
ZnSe PC-299 **2021**, *Nano Res.* Ref. 52	• IP samples from the $Zn(OAc)_2$/OLA + SeTOP + $HPPh_2$ reaction in OLA, purified with Tol and MeOH • XPS, Zn_2Se_1 (based on Zn 2p and Se 3d regions) • EDS, Zn_2Se_1 • MALDI-TOF MS, ~3350 Da, $Zn_{32}Se_{16}$

The three references are referred to those cited in the main text.

[40] T. Zhu, B. Zhang, J. Zhang, J. Lu, H. Fan, N. Rowell, J. A. Ripmeester, S. Han, K. Yu, Two-Step Nucleation of CdS Magic-Size Nanocluster MSC-311, *Chem. Mater.* **2017**, *29*, 5727−5735.

[45] M. Liu, K. Wang, L. Wang, S. Han, H. Fan, N. Rowell, J. A. Ripmeester, R. Renoud, F. Bian, J. Zeng, K. Yu, Probing Intermediates of the Induction Period Prior to Nucleation and Growth of Semiconductor Quantum Dots, *Nat. Commun.* **2017**, *8*, 15467.

[52] X. Yang, M. Zhang, Q. Shen, Y. Li, C. Luan, K. Yu, The Precursor Compound of Two Types of ZnSe Magic-sized Clusters, *Nano Res.* **2021**. DOI: 10.1007/s12274-021-3503-z.

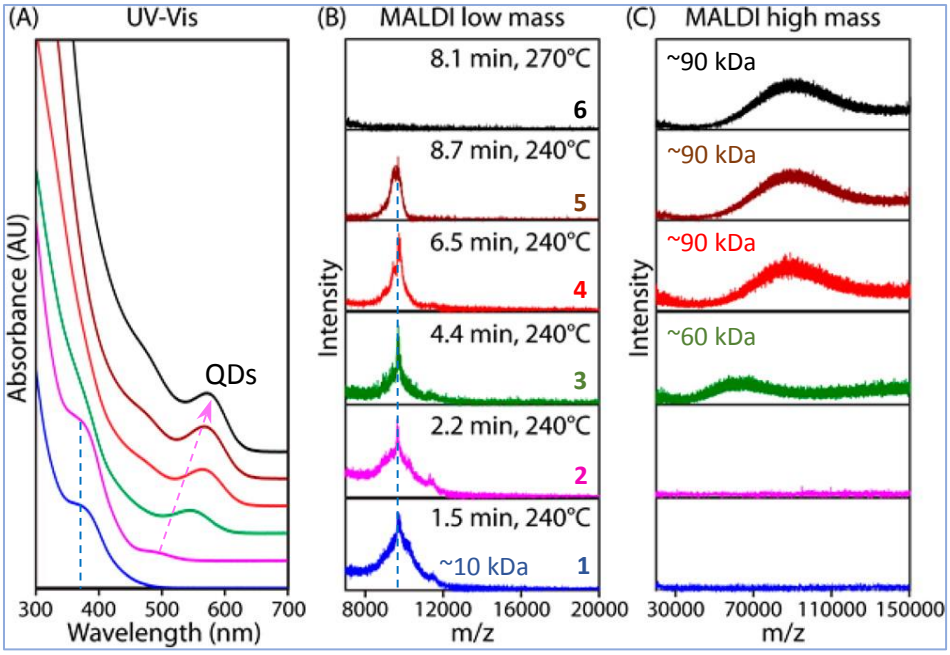

Figure S1. Derived from **Figure 2** of Ref 59 in the main text. With the two-pathway model (Scheme 1), a different perspective can be provided for the reaction. At 240 °C/1.5 min (Sample 1), the reaction was still in its prenucleation stage and the PC/MSC appeared (dashed lines). As the reaction proceeded beyond the prenucleation stage, QDs grew (dashed arrows) while the PC/MSC disappeared at 270 °C/8.1 min (Sample 6).

[59] L. Xie, Y. Shen, D. Franke, V. Sebastián, M. G. Bawendi, K. F. Jensen, Characterization of Indium Phosphide Quantum Dot Growth Intermediates Using MALDI-TOF Mass Spectrometry, *J. Am. Chem. Soc.* **2016**, *138*, 13469−13472.

Table S3. Summary of the experimental conditions for the QDs/MSCs dealt with in Part 3.

Figures, products	Reaction conditions
1a-d CdS QDs	$4Cd(OA)_2$ + 1S, [S] = 30 mmol/kg, in ODE, 160 °C/30 min, TOPO added at room temperature
1e CdS QDs	$4Cd(OA)_2$ + 1S, [S] = 30 mmol/kg, in ODE, TOPO added after (e1) and before (e2) the PC formation, 160 °C/10 min
1f CdS QDs	$4Cd(OA)_2$ + 1S + $4HPPh_2$, [S] = 30 mmol/kg, in ODE, 120 °C, TOPO added to f1 but not to f2, 120 °C/60 min
2a-b CdS MSC-311	$4Cd(OA)_2$ + 1S, [S] = 30 mmol/kg, in ODE, 180 °C/20 min
2c-d CdTe dMSC-371	$4Cd(OAc)_2$/OLA + 1TeTOP, [Te] = 44 mmol/kg, in OLA, 140 °C/20 min
3a-b CdS MSC-311	$4Cd(OA)_2$ + 1S, [S] = 30 mmol/kg, in ODE, 180 °C, MSA added at 15 min (3a) and 30 min (3b)
3c-d CdSe dMSC-393 dMSC-460	$4Cd(MA)_2$ + 1Se, [Se] = 30 mmol/kg, in ODE, 120 °C/2 h, HOAc added, 120 °C to 240 °C
4a-b CdS MSC-311 MSC-322	$4Cd(OA)_2$ + 1S + $4HPPh_2$, in ODE, 100 °C/5 min; $4Cd(OA)_2$ + 1S, in ODE, 180 °C/5 min
4c CdS MSC-311	$4Cd(MSA)_2$ + 1S and $4Cd(OA)_2$ + 1S, [S] = 30 mmol/kg, in ODE, 180 °C/75 min
4d CdTe dMSC-427	$6Cd(OA)_2$ + TeTOP + 6HOAc, [Te] = 20 mmol/kg, in ODE, 100 °C/15 min
5 CdTeSe MSC-399	$4Cd(OAc)_2$/OLA + 1ETOP (E = Se, Te), [E] = 30 mmol/kg, in OLA, 130 °C/30 min for CdTe, and 140 °C/30 min for CdSe; equal volume mixed, incubated in Tol (a-c) or dispersed in Tol and OTA mixtures (d-f)

Note S1. Experimental details and additional descriptions for Figure 1.

In Parts a to d, the CdS IP sample was prepared from a conventional reaction of $Cd(OA)_2$ and S in ODE, with a Cd to S feed molar ratio of four to one and a S concentration of 30 mmol/kg. The reaction was allowed to proceed at 160 °C for 30 min to generate CdS PCs in IP samples. The IP sample (1.0 mL) was mixed with a mixture of TOPO (0.1 g with the molar ratio of 1Cd to 2.7TOPO) and ODE (1.0 g) or with ODE (1.0 g) only at room temperature. Both of the resulting two mixtures (25 μL) were dispersed in 3.0 mL of toluene (Tol). Optical absorption spectra were collected immediately upon dispersion (a) and later after a five-day incubation in Tol (b).

In Part a, the two spectra (traces 1 and 2) are relatively featureless. In Part b, trace 1 (with TOPO added) exhibits a broad absorption peak centered around 320 nm, indicating the presence of CdS QDs. Trace 2 (without TOPO added) contains a distinct absorption peak at 311 nm, suggesting the evolution of CdS MSC-311 and the presence of PC-311 in trace 2 of Part a. For the dispersion containing TOPO, it appears that PC-311 was decomposed, which led to the absence of MSC-311 but instead the nucleation and growth of ultrasmall QDs at room temperature.

In Part e, two reaction batches were compared in detail. Both of the two reactions had been subjected to identical thermal processing. For one batch, the addition of S to $Cd(OA)_2$ was performed at 90 °C (trace 1); for the other batch, the addition concerned both S and TOPO (trace 2). After the reactions had been heated to 160 °C for 30 min, their temperatures were decreased to 120 °C. TOPO (with the feed molar ratio of 1Cd to 2.2TOPO) was added to the former batch (trace 1). Then, their temperatures were both increased to 220 °C in steps of 20 °C, with samples taken after 10 min had elapsed at each temperature.

In Part f, two reactions of $Cd(OA)_2$ + S + $HPPh_2$ in ODE are shown, which had the Cd to S to $HPPh_2$ feed molar ratios of four to one to four and the S concentration of 30 mmol/kg. Both reactions were heated to 120 °C, and TOPO was added to one of them (trace 1). Afterwards, samples were extracted after 10 to 60 min had elapsed at this temperature. An aliquot (10 μL) of each sample from the two reactions was dispersed in 6.0 mL of Tol; after one day, absorption spectra were collected. The absorption spectra of the 60 min samples are shown in Part f, where trace 1 was obtained from the sample with the addition of TOPO and trace 2 from the

sample without TOPO.

Figure 1 demonstrates that the nucleation and growth of ultrasmall CdS QDs with enhanced particle yield can occur via the TOPO-enabled fragmentation of the PCs in the CdS IP samples at low temperature. Such nucleation and growth proceed through PCs, then Mo/Fr, and finally to QDs. For the nucleation and growth of small-size CdSe and CdTe QDs, we found according to our preliminary study that the TOPO enabling process does not function in a similar way. At present, we are actively exploring a capability that will allow us to have a general, efficient control of the two proposed pathways.

Note S2. Experimental details and additional descriptions for Figure 2.

Figure 2 presents two examples of the two-step approach to binary MSCs at relatively low temperatures, showing the optical absorption and kinetic exploration for the transformation of binary CdS PCs to MSC-311 in Parts a and b, as well as that of binary CdTe PCs to dMSC-371 in Parts c and d, respectively. In Parts a and b, the CdS IP sample was prepared with the same reaction as that shown in Part a of Figure 1, but heated at 180 °C for 20 min. After the resulting IP sample was stored at −196 °C for 2 days, it (27.8 mg) was dispersed in 3.00 mL of Tol at room temperature. Optical absorption spectra were collected *in situ* in durations up to 196 min with an interval of 4 min to monitor the evolution from CdS PC-311 to MSC-311.

In Part a, after in Tol for 4 min (red trace), there is a broad absorption centering at ~302 nm, which indicates the onset of possible transformation to MSC-311. Afterwards, a continuous redshift of the absorption peak position together with the incessant increase of the peak strength appears. Along with the increase of the absorbance at about 311 nm, a correlated and noticeable decrease of the absorbance at 290 nm is observed. After 180 min, the peak is fixed at about 311 nm.

In Part b, the abscissa is the time scale in min, and the ordinate contains the absorption strength of at 311 nm at a given elapsed time (Time) (solid circle symbols). The value of A was corrected by a background absorbance, which is the value at 311 nm of the 4 min sample. The insert of Part b shows the time dependent $\ln(A^{\infty} - A)$ (open circles, where A^{∞} represents the initial amount of CdS PC-311 calculated) only up to 120 min, for the reason that the change in absorbance beyond 120 min is below the absorbance sensitivity limit (0.001). The time-dependent strength (A) follows the first-order reaction kinetics (solid curve), which obeys the equation of A = 0.411 – 0.417*exp(-0.015t) with a rate constant of 0.015 min^{-1}. With A^{∞} value of 0.411 according to the fitted equation above, the fitted trace (insert of Part b) matches well with the experimental data. In addition, it is proposed that CdS PC-311 transforms to MSC-311 via the intra-molecular reactions. MALDI-TOF mass spectra collected from one as-synthesized PC-311 sample before and after 3 days of storage (that is MSC-311) in Tol both exhibit molecular ion peaks at about m/z 5167. PC-311 and MSC-311 form a pair of quasi-isomers. By the way, the thermally-induced reversible transformation among MSC-311 and MSC-322 was

also found via incubation of CdS IP samples at different temperatures. This reversible transformation also follows the first-order reaction kinetics.

In Parts c and d, The CdTe IP sample was made from a reaction of $Cd(OAc)_2$/OLA and TeTOP in OLA with Cd to Te feed molar ratio of four to one and a Te concentration of 44 mmol/kg. After heating at 140 °C for 20 min, 30 µL of the resulting IP sample was dispersed in a mixture containing 2.95 mL of Tol and 0.05 mL of OTA. Part c shows the optical absorption spectra that were collected *in situ* over a period of 1 min to 1370 min. In the first 20 min, no significant characteristic peak is found from the time-resolved optical spectra. While in the following 180 min, the absorption peaking at 371 nm develops slowly. After 200 min, the characteristic absorption doublet peaking at ~350/371 nm increases until 1200 min had elapsed, and then maintains a nearly constant intensity.

Part d shows the kinetic studies of the development of CdTe dMSC-371, this process exhibits the first-order kinetics only after 200 min. A fitted curve A = 0.334 – 0.334*exp(-0.004t) was obtained with a rate constant of 0.004 min^{-1}. The inset of Part d shows that the fitted line matches well with the data of time-dependent $\ln(A^{\infty} - A)$ (open circles, with $A^{\infty} = 0.334$), supporting the first-order reaction kinetics transformation behavior. It should be noted that the transformation from binary PCs to binary MSCs does not always follow first-order kinetics probably due to the as-synthesized PC (in an IP sample) and the immediate PC (in an incubated and/or diluted sample) are different. It is reasonable to consider that, the immediate PC transforms to CdTe dMSC-371 following the first-order kinetics via an intra-molecular reaction after 200 min. Before that, the as-synthesized PC (1 min in Part c) gradually develops to immediate PC.

Note S3. Experimental details and additional descriptions for Figure 3.

For Parts a and b, the CdS sample was prepared with the same reaction as that shown in Parts a and b of Figure 2, but maintained a constant temperature at 180 °C. 1.75 mmol of branched 2-methyloctadecanoic acid ($(C_{16}H_{33}CH(CH_3)$-COOH, MSA) was added to the CdS samples at 15 min (blue trace) and 30 min (red trace). For the 15 min addition batch (a), 10 samples were taken at (1) 15, (2) 20, (3) 30, (4) 35, (5) 45, (6) 60, (7) 75, (8) 90, (9) 120, and (10) 135 min. For the 30 min addition batch (b), 8 samples were taken at (1) 30, (2) 35, (3) 45, (4) 60, (5) 75, (6) 90, (7) 120, and (8) 135 min. The resulting samples (25 μL) were dispersed in 3.00 mL Tol for the immediate absorption measurements. Because the induction period lasts at least 15 min in this reaction, thus here we exactly compare the effect of addition of MSA before (Part a) and after (Part b) the nucleation and growth of QDs. For the former, MSC-311 increases steadily within 120 min and reaches the optical density of 1.04 at 120 min (trace 9 of part a). For the latter batch, the QDs keep growing and exhibit broad absorption peaks, while the initial presence of MSC-311 (before 60 min) decreases and disappears. It is unclear, on a molecular level, how the nucleation and growth of QDs was significantly suppressed when MSA was added in the prenucleation stage (Part a). After the QDs appeared in the reaction (Part b), the presence of MSA did not prevent the growth of QDs, which resulted in the fragmentation of the PCs.

Parts c and d show the presence of short-chain acetic acid (HOAc) in the prenucleation stage could obtain the production of photoluminescence CdSe MSCs without the co-production of QDs. The CdSe IP sample was prepared from cadmium myristic ($Cd(OOC(CH_2)_{12}CH_3)_2$, $Cd(MA)_2$, made from CdO) and Se with a feed molar ratio of four to one and a Se concentration of 30 mmol/kg in ODE. The reaction temperature was increased from room temperature to 120 °C and kept at this temperature for 2 h. Then, 5.00 mmol HOAc was added and kept for 15 min (trace 1), followed by increasing the reaction temperature in steps of 20 °C. Samples were extracted at each temperature step after 15 min had elapsed. There are eight spectra collected: traces 1 to 8 respectively refer to samples of 120 °C/15 min to 240 °C/15 min, except that the traces 7 represent the 240 °C/0 min sample. Each sample (15 μL) was dispersed in 3.00 mL of

Tol for spectroscopy study. The photoluminescence (PL) spectra were operated under excitation wavelength of 350 nm.

In Part c, CdSe dMSC-393 (with an absorption doublet at 372/392 nm) and dMSC-460 (with a sharp absorption doublet at 433/461 nm) are produced at 180 °C (Part c, trace 4). The trace 4 exhibits main emission peaking at about 399 nm (Part d). When the reaction temperature is increased to 240 °C, the population of dMSC-460 increases and dMSC-393 disappears, together with a single emission peaking at about 465 nm without broad trap emission. Note that no QDs is produced even at 240 °C during the temperature increases. In this case of addition HOAc, $Cd(MA)_2$ and HOAc interact to produce MA-Cd-OAc.

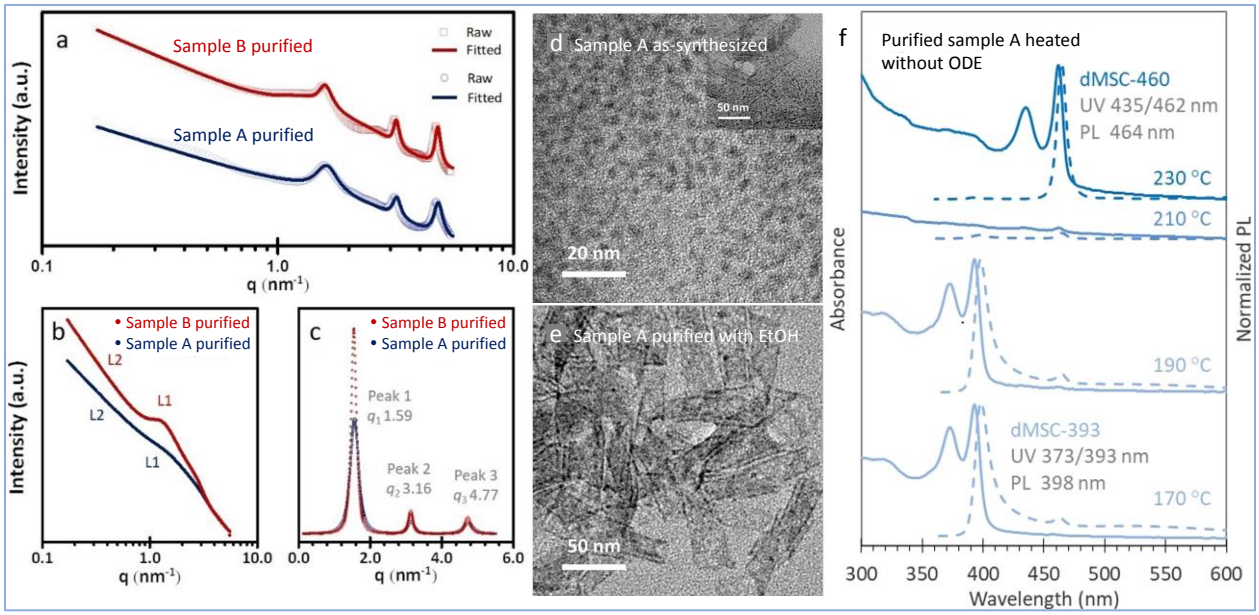

Figure S2. Derived from **Figures 4, S1-2** and **1** of Ref 35 in the main text.

- (a to c) SAXS of CdSe dMSC-393 and NPL-393 (190 °C/5 min Sample A purified, blue traces) and CdSe dMSC-460 and NPL-460 (230 °C/30 min Sample B purified, red traces). The purification did not use C_2H_5OH (EtOH) but toluene only; purified Samples A and B were kept for seven days before the SAXS measurements performed. SAXS suggests that dMSC-393 and dMSC-460 are disc-shaped and have the respective radii of gyration (R_g) of 0.92 and 1.14 nm. Moreover, dMSC-393 and dMSC-460 assembled into multilayered nanostructures, NPL-393 and NPL-460, with the same layered spacing of $2\pi/q_1$. The self-assemble occurred mainly during the seven-day storage, we believe.
- (d and e) TEM images of as-synthesized (d) and purified (e) Sample A. C_2H_5OH was used in purification, and the self-assembly of the zero-dimension dMSC-393 resulted the two-dimension nanoplatelets (NPL-393) (e). In a side note, the TEM and XRD studies for zero-dimension dMSC-460 and two-dimension NPL-460 are available elsewhere.[1-6] Hopefully, these experimental data from Yu and coworkers, including those for CdTe and CdS,[7-10] will encourage a reconsideration of the assignment for the nanospecies that display similar optical absorption and PL spectra.[11-14]
- (f) Optical spectroscopy study of purified Sample A when it was heated. The purification used toluene only.

[1] J. Zhu, Z. Cao, Y. Zhu, N. Rowell, Y. Li, S. Wang, C. Zhang, G. Jiang, M. Zhang, J. Zeng, K. Yu, Transformation Pathway from CdSe Magic-Size Clusters with Absorption Doublets at 373/393 nm to Clusters at 434/460 nm, *Angew. Chem. Int. Ed.* **2021**, *60*, 20358−20365.

[2] Y. Liu, B. Zhang, H. Fan, N. Rowell, M. Willis, X. Zheng, R. Che, S. Han, K. Yu, Colloidal CdSe 0-Dimension Nanocrystals and Their Self-Assembled 2-Dimension Structures, *Chem. Mater.* **2018**, *30*, 1575−1584.

[3] Y. Liu, M. Willis, N. Rowell, W. Luo, H. Fan, S. Han, K. Yu, Effect of Small Molecule Additives in the Prenucleation Stage of Semiconductor CdSe Quantum Dots, *J. Phys. Chem. Lett.* **2018**, *9*, 6356–6363.

[4] Y. Liu, N. Rowell, M. Willis, M. Zhang, S. Wang, H. Fan, W. Huang, X. Chen, K. Yu, Photoluminescent Colloidal Nanohelices Self-Assembled from CdSe Magic-Size Clusters via Nanoplatelets, *J. Phys. Chem. Lett.* **2019**, *10*, 2794−2801.

[5] K. Yu, J. Ouyang, M. B. Zaman, D. Johnston, F. J. Yan, G. Li, C. I. Ratcliffe, D. M. Leek, X. Wu, J. Stupak, Z. Jakubek, D. Whitfield, Single-Sized CdSe Nanocystals with Bandgap Photoemission via a Noninjection One-Pot Approach, *J. Phys. Chem. C* **2009**, *113*, 3390–3401.

[6] J. Ouyang, M. B. Zaman, F. J. Yan, D. Johnston, G. Li, X. Wu, D. Leek, C. I. Ratcliffe, J. A. Ripmeester, K. Yu, Multiple Families of Magic-Sized CdSe Nanocrystals with Strong Bandgap Photoluminescence via Noninjection One-Pot Syntheses, *J. Phys. Chem. C* **2008**, *112*, 13805–13811.

[7] R. Wang, J. Ouyang, S. Nikolaus, L. Brestaz, M. B. Zaman, X. Wu, D. Leek, C. I. Ratcliffe, K. Yu, Single-Sized Colloidal CdTe Nanocrystaks with Strong Bandgap Photoluminescence, *Chem. Commun.* **2009**, *113*, 962−964.

[8] M. Chen, C. Luan, M. Zhang, N. Rowell, M. Willis, C. Zhang, S. Wang, X. Zhu, H. Fan, W. Huang, K. Yu, B. Liang, Evolution of CdTe Magic-Size Clusters with Single Absorption Doublet Assisted by Adding Small Molecules during Prenucleation, *J. Phys. Chem. Lett.* **2020**, *11*, 2230−2240.

[9] M. Li, J. Ouyang, C. I. Ratcliffe, L. Pietri, X. Wu, D. M. Leek, I. Moudrakovski, Q. Lin, B. Yang, K. Yu, CdS Magic-Sized Nanocrystals Exhibiting Bright Band Gap Photoemission via Thermodynamically Driven Formation, *ACS Nano* **2009**, *3*, 3832−3838.

[10] Z. He, D. Wang, Q. Yu, M. Zhang, S. Wang, W. Huang, C. Luan, K. Yu, Evolution of Photoluminescent CdS Magic-Size Clusters Assisted by Adding Small Molecules with Carboxylic Group, *ACS Omega* **2021**, *6*, 14458−14466.

[11] J. Joo, J. S. Son, S. G. Kwon, J. H. Yu, T. Hyeon, Low-Temperature Solution-Phase Synthesis of Quantum Well Structured CdSe Nanoribbons, *J. Am. Chem. Soc.* **2006**, *128*, 5632–5633.

[12] S. Ithurria, B. Dubertret, Quasi 2D Colloidal CdSe Platelets with Thicknesses Controlled at the Atomic Level, *J. Am. Chem. Soc.* **2008**, *130*, 16504–16505.

[13] Y. Ren, D. Chen, Z. Li, X. Peng, Symmetry-Breaking for Formation of Rectangular CdSe Two-Dimensional Nanocrystals in Zinc-Blende Structure, *J. Am. Chem. Soc.* **2017**, *139*, 10009–10019.

[14] A. Riedinger, F. D. Ott, A. Mule, S. Mazzotti, P. N. Knüsel, S. J. P. Kress, F. Prins, S. C. Erwin, D. J. Norris, An Intrinsic Growth Instability in Isotropic Materials Leads to Quasi-Two-Dimensional Nanoplatelets, *Nat. Mater.* **2017**, *16*, 743–748.

Note S4. Experimental details and additional descriptions for Figure 4.

In Parts a and b, the CdS samples were synthesized from $Cd(OA)_2$ + S + $HPPh_2$ at 100 °C (reaction 1, traces 1) and $Cd(OA)_2$ + S at 180 °C (reaction 2, traces 2), both with a Cd to S feed molar ratio of four to one and a S concentration of 30 mmol/kg. The feed molar ratio of $HPPh_2$ to S (traces 1) is also four to one. First, each of the two reactions was held at 40 °C for 10 min with one sample extracted. Afterward, the reaction temperature was increased to 100 °C for reaction 1 and to 180 °C for reaction 2. The reaction periods were 5 min as indicated. The samples (10 µL each) from reaction 1 were dispersed in 6.0 mL of Tol, while samples (25 µL each) from reaction 2 were dispersed in 3.0 mL of Tol. The absorption measurements were performed before (Part a) and after (Part b) a one-day incubation. The data of reaction 1 have been multiplied by a factor of five for comparison with reaction 2.

In Parts a and b, for the reaction 1 at 100 °C for 5 min, MSC-322 evolves at 0 day (trace 1 of Part a, with the optical density of 1.40). After a one-day incubation, a majority of CdS MSC-322 transforms to CdS MSC-311 (via their corresponding PC) with little change in absorption intensity. It has been demonstrated that the onset of the Cd-S bond was at ~140 °C for the reaction of $Cd(OA)_2$ and S in ODE (see the description of Step 2 in the Introduction). These results suggest that a lower temperature is needed for the covalent-bond formation of MSCs in the presence of $HPPH_2$. For the reaction 2 at 180 °C for 5 min, the 0-day sample is featureless, but exhibits a characteristic peaking at about 311 nm after a one-day room temperature incubation, indicating that CdS PC-311 transforms to MSC-311 via incubation. In this regard, a two-step based selective approach is needed for the formation of CdS MSCs (trace 2) under this condition. The utilization of $HPPh_2$ results in a higher production yield of MSCs for reaction 1 at 100 °C than that of the reaction 2 at 180 °C, while accompanying with the co-production of very small amount of QDs.

In Part c, for the reaction of $Cd(OA)_2$ + S, CdO, OA and ODE were mixed for the preparation of Cd precursors, together with S powder as the S precursors. For the reaction of $Cd(MSA)_2$ + S, only OA was replaced by MSA. Then, the resulting two reactions were heated to 180 °C for 75 min. Each sample (25 µL) was dispersed in 2.95 mL Tol and 0.05 mL MeOH for the absorption measurements. The reaction of $Cd(OA)_2$ + S exhibits a broad absorption peak around 387 nm,

suggesting the formation of CdS QDs. The reaction of $Cd(MSA)_2$ + S shows a single and sharp absorption peak at 309 nm, suggesting the formation of MSC-311 without any contamination of QDs.

In Part d, the presence and absence of HOAc in the reaction of $Cd(OA)_2$ + TeTOP in ODE are shown. The reaction had the Cd to Te (to HOAc) feed molar ratio of six to one (to six) and the Te concentration of 20 mmol/kg. TeTOP was added to the mixture of $Cd(OA)_2$ and ODE at 40 °C with (trace 1) and without (trace 2) the presence of HOAc. Then, the temperatures of two reactions were increased to 100 °C in steps of 20 °C and kept at 100 °C for 15 min. 10 µL of the resulting mixture was dispersed in 3.0 mL of Tol for the spectroscopy study. The inset of Part d shows the TEM image of the as-synthesized 40 min sample from another batch without any sampling. This batch was the same as the Part d, but at a constant temperature of 100 °C. Evidently, the presence of HOAc results in the evolution of CdTe dMSC-427 (exhibiting a double absorption peaking at 383 and 425 nm) in a single-ensemble form. Without HOAc, the only production of QDs with a broad absorption peak at 490 nm are observed. The reason for the difference might be related to the reaction of $Cd(OA)_2$ + HOAc $\Leftrightarrow$ $Cd(OA)_1(OAc)_1$ + HOA. $Cd(OA)_2$ has a relatively high solubility, and $Cd(OA)_1(OAc)_1$ has a relatively low solubility. They favor the formation of QDs and dMSC-427, respectively.

Note S5. Experimental details and additional descriptions for Figure 5.

In Parts a to c, CdTe IP samples and CdSe IP samples were prepared from $Cd(OAc)_2$/OLA + TeTOP and $Cd(OAc)_2$/OLA + SeTOP, respectively. All the IP samples were synthesized with a feed molar ratio of 4Cd to 1E (E = TeTOP or SeTOP) and a Cd concentration of 120 mmol/kg in OLA. The resulting mixtures were heated for 30 min at the desired temperature (130 °C for CdTe IP samples, and 140 °C for CdSe IP samples). CdTe and CdSe IP samples were mixed at room temperature with an equal volume for the formation of CdTeSe MSC-399 after a 43-h incubation. An aliquot (30 μL) of each sample before (blue traces) and after (red traces) incubation was dispersed in Tol for the optical absorption measurements.

In Parts a to c, all the blue traces are transparent in absorption spectra, suggesting that no MSC formed before incubation. In Parts a and b, the samples after a 43-h incubation (red traces) show the distinct narrow absorption, exhibiting characteristic peaking at 349/369 nm, 415 nm, respectively. These results support that CdTe dMSC-371, CdSe MSC-415 were formed (from their corresponding PCs) after incubation. In Part c, the red trace exhibits a sharp absorption singlet peaking at 398 nm without the emergence of other-bandgap MSCs and QDs, indicating the formation of CdTeSe MSC-399. As a side note, the comparison experiments of mixing CdTe (130 °C/30 min) samples with SeTOP or mixing CdSe (140 °C/30 min) samples with TeTOP indicated that no anion exchange reaction (with SeTOP or TeTOP) took place at room temperature. Only one optical absorption peak at 398 nm evolves from the binary mixture after incubation, suggesting that the CdTe PC to MSC-371 and CdSe PC to MSC-415 transformations do not take place, but the substitution reactions do, together with the CdTeSe PC to MSC-399 transformation. Besides, as suggested by synchrotron-based *in situ* SAXS, the size of a binary mixture obtained is similar to those of corresponding binary CdTe and CdSe. It is noteworthy that CdTeSe alloy MSC-399 was not engineered from a reaction consisting of $Cd(OAc)_2$/OLA, TeTOP, and SeTOP with heating up approach.

In Parts d to f, the as-mixed sample (with just a one-minute incubation) was dispersed in the mixture containing 2.5 mL Tol and 0.5 mL OTA (Parts d and e) or 2.0 mL Tol and 1.0 mL OTA (Part f). In Part f, the absorption spectra were collected after dispersion for 1 min to 4 h. The presence of an absorption peaking at about 371 nm at 1 min indicates the presence of CdTe

MSC-371. It is worth noting that, another absorption peaking at about 399 nm raises up accompanying with the decrease of peaking at 371 nm.

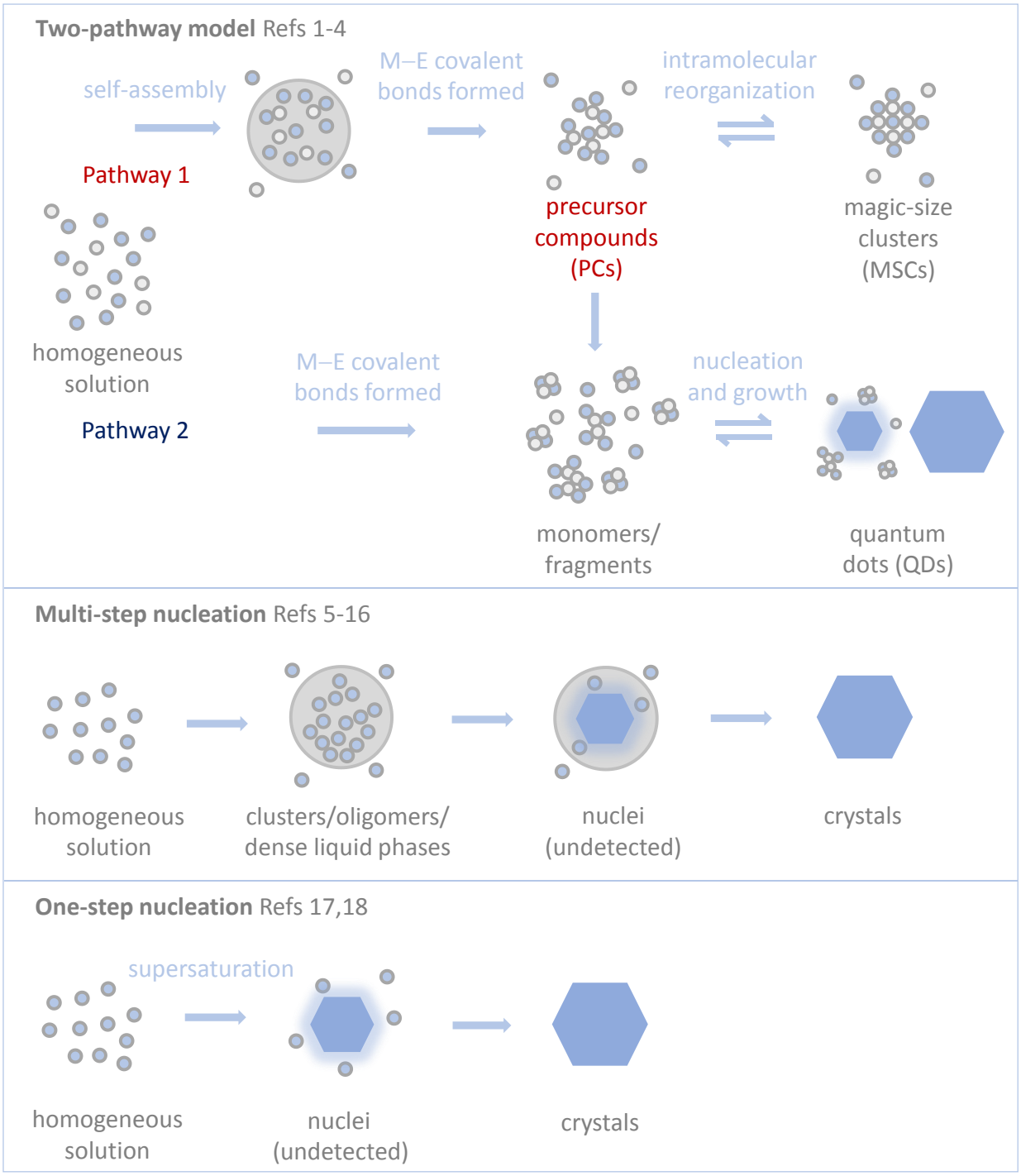

Scheme S4. Schematic drawing to illustrate the comparison of the proposed nucleation models. The size scale is not considered. (Top panel) The two-pathway model is proposed to understand

the nucleation/growth of colloidal semiconductor QDs.[1-4] When a reaction contains sufficient M and E precursors, their self-assembly (Pathway 1) is active. However, when their concentrations are sufficiently low, Pathway 1 is suppressed and the nucleation and growth of QDs goes through Pathway 2 only; the product does not contain the PC.[3,4] We remind that the PC is identified as an intermediate that can result in the occurrence of the MSC, and a single PC can transform into a single MSC; this one-to-one relationship is noteworthy. (Middle panel) The multi-step model within non-classical nucleation theories has been applied for organic molecules,[5-8] proteins,[9,10] calcium-based inorganics,[11-13] and metals.[14-16] In these cases the self-assembly process results in the occurrence of dense liquid droplets, as detailed by the description "An amorphous phase is rapidly aggregated from the homogeneous solution."[15] Meanwhile, how oil droplets and the nuclei within are related has not been well understood. The questions include, for example, how many nuclei form inside a single dense liquid droplet, and whether a single crystal grows from a single dense liquid droplet.[14,15] (Bottom panel) The one-step model addressed in classical nucleation theory (CNT) was reported recently to work for ice formation.[17,18]

[1] M. Liu, K. Wang, L. Wang, S. Han, H. Fan, N. Rowell, J. A. Ripmeester, R. Renoud, F. Bian, J. Zeng, K. Yu, Probing Intermediates of the Induction Period prior to Nucleation and Growth of Semiconductor Quantum Dots, *Nat. Commun.* **2017**, *8*, 15467.

[2] J. Zhang, X. Hao, N. Rowell, T. Kreouzis, S. Han, H. Fan, C. Zhang, C. Hu, M. Zhang, K. Yu, Individual Pathways in the Formation of Magic-Size Clusters and Conventional Quantum Dots, *J. Phys. Chem. Lett.* **2018**, *9*, 3660-3666.

[3] L. Wang, J. Hui, J. Tang, N. Rowell, B. Zhang, T. Zhu, M. Zhang, X. Hao, H. Fan, J. Zeng, S. Han, K. Yu, Precursor Self-Assembly Identified as a General Pathway for Colloidal Semiconductor Magic-Size Clusters, *Adv. Sci.* **2018**, *5*, 1800632.

[4] C. Palencia, K. Yu, K. Boldt, The Future of Colloidal Semiconductor Magic-Size Clusters, *ACS Nano* **2020**, *14*, 1227-1235.

[5] R. J. Davey, S. L. Schroeder, J. H. Horst, Nucleation of Organic Crystals—A Molecular Perspective, *Angew. Chem. Int. Ed.* **2013**, *52*, 2166–2179.

[6] H. Chen, M. Li, Z. Lu, X. Wang, J. Yang, Z. Wang, F. Zhang, C. Gu, W. Zhang, Y. Sun, J. Sun, W. Zhu, X. Guo, Multistep Nucleation and Growth Mechanisms of Organic Crystals from Amorphous Solid States, *Nat. Commun.* **2019**, *10*, 3872.

[7] E. Wiedenbeck, M. Kovermann, D. Gebauer, H. Colfen, Liquid Metastable Precursors of Ibuprofen as Aqueous Nucleation Intermediates, *Angew. Chem. Int. Ed.* **2019**, *58*, 19103–19109.

[8] H. Chen, W. Zhang, S. Ren, X. Zhao, Y. Jiao, Y. Wang, J. F. Stoddart, X. Guo, Temperature-Triggered Supramolecular Assembly of Organic Semiconductors, *Adv. Mater*. **2021**, 2101487.
[9] M. Sleutela, A. E. S. van Driessche, Role of Clusters in Nonclassical Nucleation and Growth of Protein Crystals, *Proc. Natl. Acad. Sci.* **2014**, *111*, 546–553.
[10] X. Ma, S. Zhang, F. Jiao, C. J. Newcomb, Y. Zhang, A. Prakash, Z. Liao, M. D. Baer, C. J. Mundy, J. Pfaendtner, A. Noy, C. Chen, J. J. De Yoreo, Tuning Crystallization Pathways through Sequence Engineering of Biomimetic Polymers, *Nat. Mater.* **2017**, *16*, 767–774.
[11] D. Gebauer, A. Völkel, H. Cölfen, Stable Prenucleation Calcium Carbonate Clusters, *Science* **2008**, *322*, 1819-1822.
[12] A. Dey, P. H. H. Bomans, F. A. Müller, J. Will, P. M. Frederik, G. de With, N. A. J. M. Sommerdijk, The Role of Prenucleation Clusters in Surface-Induced Calcium Phosphate Crystallization, *Nat. Mater.* **2010**, *9*, 1010–1014.
[13] Z. Liu, C. Shao, B. Jin, Z. Zhang, Y. Zhao, X. Xu, R. Tang, Crosslinking Ionic Oligomers as Conformable Precursors to Calcium Carbonate, *Nature* **2019**, *574*, 394–398.
[14] N. D. Loh, S. Sen, M. Bosman, S. F. Tan, J. Zhong, C. A. Nijhuis, P. Král, P. Matsudaira, U. Mirsaidov, Multistep Nucleation of Nanocrystals in Aqueous Solution, *Nat. Chem.* **2017**, *9*, 77–82.
[15] J. Yang, J. Koo, S. Kim, S. Jeon, B. K. Choi, S. Kwon, J. Kim, B. H. Kim, W. C. Lee, W. B. Lee, H. Lee, T. Hyeon, P. Ercius, J. Park, Amorphous-Phase-Mediated Crystallization of Ni Nanocrystals Revealed by High-Resolution Liquid-Phase Electron Microscopy, *J. Am. Chem. Soc.* **2019**, *141*, 763–768.
[16] B. Jin, Y. Wang, Z. Liu, A. France-Lanord, J. C. Grossman, C. Jin, R. Tang, Revealing the Cluster-Cloud and Its Role in Nanocrystallization, *Adv. Mater.* **2019**, *31*, 1808225.
[17] V. K. LaMer, R. H. Dinegar, Theory, Production and Mechanism of Formation of Monodispersed Hydrosols, *J. Am. Chem. Soc.* **1950**, *72*, 4847–4854.
[18] G. Bai, D. Gao, Z. Liu, X. Zhou, J. Wang, Probing the Critical Nucleus Size for Ice Formation with Graphene Oxide Nanosheets, *Nature* **2019**, *576*, 437−441.